

# UNIVERSITY OF ARIZONA

## Nuclear Fuel Cycle Research Program

PROGRESS REPORT

NRC-04-86-114

UNSATURATED FLOW AND TRANSPORT THROUGH FRACTURED ROCK  
RELATED TO HIGH-LEVEL WASTE REPOSITORIES

SUBMITTED TO: Thomas J. Nicholson, Project Manager  
U.S. Nuclear Regulatory Commission  
Office of Research  
Division of Engineering Safety  
and Earth Sciences  
Washington, D.C. 20555

SUBMITTED BY: Daniel D. Evans, Principal Investigator  
Department of Hydrology and Water Resources  
University of Arizona, Tucson, AZ 85721

November 1, 1987

HYDROLOGY DOCUMENT NUMBER 211

This report summarizes research activities conducted by the University of Arizona as part of US NRC Contract 04-86-114 for the period July 1, 1986 to October 31, 1987. The activities have progressed on topics related to work tasks as specified under the contract. The specific objectives of the contract are the determination of:

1. Methods for estimating and controlling uncertainties in sub-surface hydrologic testing and monitoring equipment,
2. Sub-surface instrument emplacement strategies and the importance of scale effects,
3. Characterization techniques for matrix and fracture systems,
4. Methods to analyze flux and travel times in fracture-matrix systems,
5. Appropriate computer models for vapor-liquid flow systems,
6. Methods for sampling liquid and vapor in the unsaturated zone,
7. Ground-water recharge, infiltration and deep percolation techniques, and
8. Calibration strategies of field site conditions using ground-water chemistry.

Only three aspects of the research conducted during the period are reported in this document. The first two aspects are related to Tasks 2 and 3, listed above, while the third aspect is related to Task 7. The first aspect summarized in this document is a description of the calibration of neutron count measurements to rock water content. The second section describes characterization techniques for an unsaturated rock matrix. Data from oriented cores are examined to determine the spatial variability of physical, hydraulic and pneumatic parameters, as well as to evaluate the precision of measurement techniques. The final section provides a description of a field site and a proposed strategy for developing techniques to estimate infiltration, deep percolation, and recharge potentials of atmospheric precipitation falling on fractured rock within arid land regions.

Another accomplishment during the report period is the development of a document related to Task 5 which describes a proposed methodology for modeling fluid flow and solute transport through the unsaturated

zone. The methodology is important for identifying important processes and parameters at the Apache Leap Tuff Site and for interpreting field data resulting from hydraulic and pneumatic testing at the site. A draft copy of this document has been recently submitted to the project monitor for review.

### Calibration of Neutron Borehole Logs

Changes in rock water content using neutron logging have been demonstrated within nine inclined boreholes with diameters of ten centimeters at the Apache Leap Tuff Site. In addition, investigations of heat flow in welded tuff by Davies (1987) using heaters placed in 5.1 cm diameter boreholes have shown long term changes in rock water content. In order to quantify these changes a theoretical calibration curve has been developed by Elder (thesis in preparation). While the calibration curve has been validated for soils, negative water contents occasionally result when using the calibration for welded tuff near the Apache Leap Test Site. Because negative water contents are impossible and also because accurate estimates of rock water contents are important, a calibration curve derived from field data was deemed necessary. The observed calibration curve is also necessary to adjust the theoretical calibration curve for differences in geometric factors, such as borehole diameter, and for differences rock bulk densities.

Estimates of the water content of porous media can be determined from counts of thermalized neutrons once a calibration curve has been obtained. Calibration curves for soils are developed by determining the neutron thermalization properties in the field or by excavating soil samples and placing the samples in large drums for measurement. In order to determine the thermalization properties, samples of the soil are either removed from the ground using a thin-walled sampler and taken to the laboratory where each sample is oven dried, or in the case of large drum measurements the amount of water added is recorded. The relationship between thermalization and water content is then determined for a number of water contents.

For rock samples the calibration is more difficult due to the difficulties associated with extracting rock samples. Existing augering and drilling methods are inappropriate for correlating field estimates of thermalization properties to water content due to the large thermal and hydraulic disturbances induced using these methods. Alternately, rock chips can be placed in large drums and the thermalization properties determined for various water contents. Substantial differences in bulk density will occur, however, due to the difficulty in repacking the rock chips to their original density.

To obtain a relationship between neutron counts and water content at the Apache Leap Tuff Site, two neutron calibration holes were excavated to a depth of 1.8 m using a pneumatic hammer. The calibration holes have a diameter of 5.1 cm and were located so that one hole was more likely to have a higher water content than the other. The wetter hole was located in the middle of an ephemeral stream channel, while the drier hole was located away from water sources other than precipitation. The locations of the neutron calibration boreholes are indicated in Figure 1. Each hole was capped with a stopper to prevent atmospheric desiccation and the dry and wet holes were allowed to equilibrate for 21 and 32 days, respectively, to allow any effects of excavation to dissipate. Representative neutron counts at various depths in the calibration holes after equilibration are presented in Table 1.

After the equilibration period, a pneumatic hammer was used to remove rock samples from the surface down to a depth of 0.42 m in the dry hole and 0.50 m in the wet hole. Upon excavation, the rock samples were immediately placed inside a collection can and weighed. Approximately twenty rock samples were removed from around each calibration hole. Each sample weighed approximately 0.150 kg. The samples were taken to the laboratory where they were oven-dried and reweighed to determine the field water content. To determine the relative saturation, porosity, and volumetric water content the samples were saturated under a vacuum, weighed under water, and reweighed while suspended under water. (The procedure is described in greater detail in the following section.) Table 2 presents the results of the analyses for rock samples extracted from the two neutron calibration boreholes.

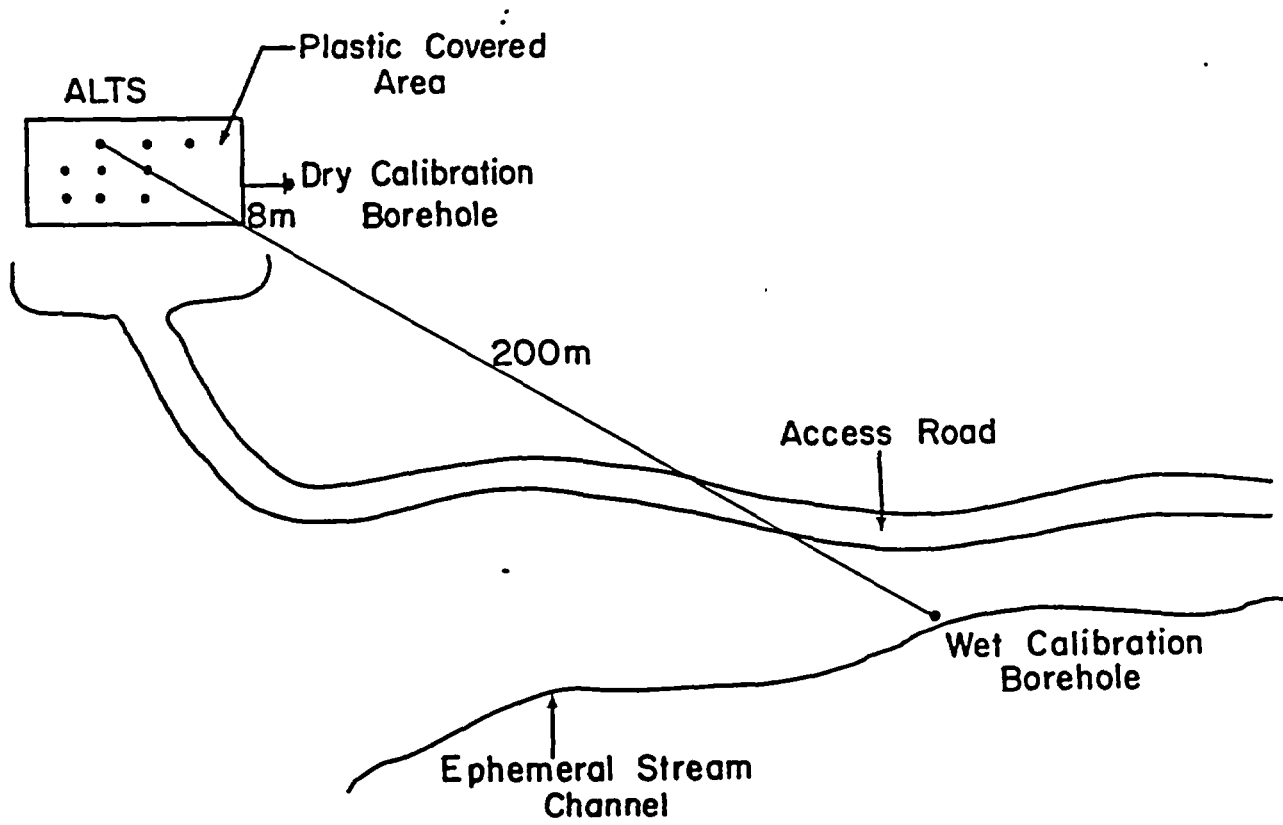


Figure 1: Location of calibration boreholes at the Apache Leap Tuff Site.

-----  
 Table 1: Observed neutron counts with depth at two calibration boreholes, Apache Leap Tuff Site. Neutron counts in the dry and wet boreholes were obtained on 10/24/87 and 11/4/87, respectively.  
 -----

Depth (cm)	Dry Borehole (Counts/120 s)	Wet Borehole (Counts/120 s)
30	63,984	81,667
40	64,252	83,370
50	64,437	82,722
60	64,417	80,722
85	65,360	84,276
110	65,263	83,639
135	65,902	79,590
160	69,567	81,417

-----  
 Table 2: Results for neutron calibration borehole tests, Apache Leap Tuff Site. Neutron measurements were obtained at a depth of 0.40 m. The dry and wet boreholes were excavated on 10/24/87 and 11/4/87, respectively.  
 -----

	<u>Dry Borehole</u>	<u>Wet Borehole</u>
Neutron Counts per 120 s	64,239 ± 80	82,547 ± 64
Bulk Density (gm/cm <sup>3</sup> )	2.13	2.09
Volumetric Water Content		
Observed	10.2 %	14.2 %
Predicted	5.8 %	10.3 %

The predicted water content in Table 2 was obtained using a nonlinear theoretical model developed by Elder. A linearized form of the nonlinear model is:

$$(1a) \quad \theta = (C - 20,415) / 202,500$$

where  $\theta$  is the water content, dimensionless, and C is the number of neutron counts per minute. A linear relationship between water content and neutron counts based upon the calibrated data is:

$$(1b) \quad \theta = (C - 8,836) / 228,300$$

It can be observed from the two equations that the slope of the linear relationship, corresponding to the denominator of the equations presented above, are very nearly the same. The change in the number of neutron counts is directly related to the change in the amount of water present, and is not expected to vary significantly between theory and field data. The observed intercept, however, is substantially different from the predicted value due to the failure of model parameters to predict the effect of the rock mass on the thermalization of neutrons. The diffusion of neutrons through a rock mass of high density is probably not described by a theory which was developed for applications involving diffusion through the lower bulk density of unconsolidated soil particles.

Additional calibration of neutron counts at various water contents within 5 and 10 cm diameter boreholes will be performed to further validate the calibration curve. A third hole in a dryer location will be drilled, monitored and excavated to validate the present empirical calibration curve and to verify the linearity of the curve over the full range of water contents expected at the Apache Leap Tuff Site.

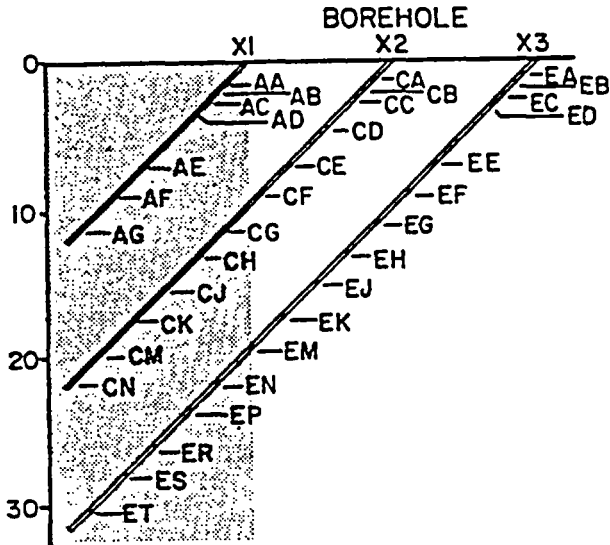
Laboratory Data Related to Oriented Borehole Core Samples

The characterization of flow and transport of fluids and solutes through the fractured tuff at the Apache Leap Tuff Site requires that relevant physical and hydrogeologic parameters be estimated. In particular, rock matrix and rock fracture characterization parameters need to be determined using field and laboratory data. The objective of this data collection program is to provide data sets for subsequent use in field scale computer simulation models of unsaturated fluid flow and solute transport. Specifically, estimates are being obtained for:

- Rock bulk density;
- Effective matrix porosity;
- Matrix pore size distribution;
- Matrix pore surface area;
- Moisture characteristic curves;
- Saturated hydraulic conductivity and relative (i.e., unsaturated) hydraulic permeabilities;
- Pneumatic conductivity and relative pneumatic permeabilities; and
- Saturated and relative thermal conductivity and thermal diffusivity.

To assure accurate and reproducible parameter estimates, a quality assurance/quality control (QA/QC) program has been established. (The program is used for all data collection activities and is not limited to this aspect.) Methods developed for obtaining parameter estimates, as well as equipment calibration and data reduction methods, are examined to ensure that consistent and verifiable procedures are employed.

The matrix parameters are obtained from core samples located at depths varying from three to thirty meters within nine inclined boreholes (Figure 2). The rock samples are collected from six centimeter diameter, oriented cores which were extracted at the time of borehole construction. The samples are removed from unfractured core sections at roughly three meter intervals along the core. Laboratory methods for determining parameters include the mercury porosimetry technique, a thermocouple psychrometer, a newly developed permeameter, and the out-flow method. These methods use rock core samples of various dimensions,



*APACHE LEAP TUFF SITE  
 CORE SAMPLE LOCATIONS*

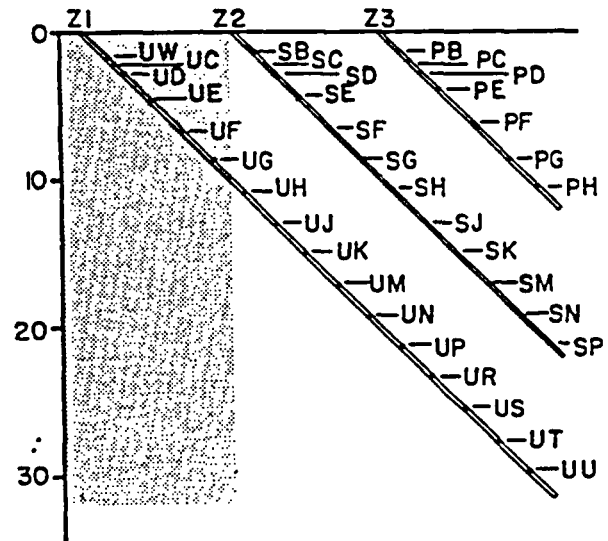
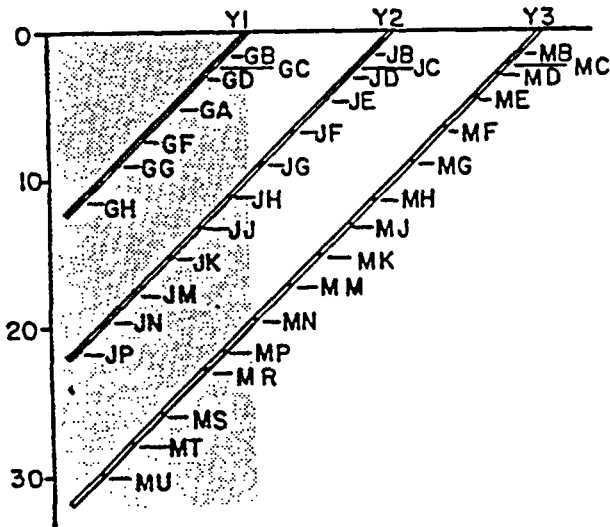


Figure 2: Location of core samples obtained from inclined boreholes (shaded area). Cores are used to characterize the physical, hydraulic, pneumatic and thermal properties of a (10 x 10 x 30 m) fractured rock block at the Apache Leap Tuff Site. Letters are codes for different sample locations.

as illustrated in Figure 3. The smallest rock core samples (approximately 1 cm in diameter and 1 cm long) are required for use in the thermocouple psychrometer, which provides the moisture characteristic curve for drier rock cores (i.e., cores with potentials greater than approximately three bars suction or water contents less than approximately 80 percent). Somewhat larger cores (approximately 2 cm in diameter and 2 cm long) are required by the mercury porosimeter in order to determine the rock pore size distribution and the pore area. Both of these cores are obtained by coring the original 5 cm diameter core. Six centimeter lengths of the original core are used to determine the remaining parameters. These parameters are described in greater detail below.

#### Effective Matrix Porosity, Pore Size Distribution and Bulk Density

The total water holding capacity of the rock matrix is limited by the porosity of the geologic medium. The matrix porosity is the amount of pore space within a rock mass, exclusive of fractures and sizable solution openings. The total matrix porosity includes pores which are isolated from other pores, while the effective matrix porosity refers only to the pores which are interconnected, and is less than or equal to the total matrix porosity. The pore size distribution, in contrast to the effective porosity, is a quantification of the effective porosity in terms of a distribution of pores with an assumed right cylindrical shape. The pore size distribution can be obtained using a mercury porosimeter (Klavetter and Peters, 1987) or the nitrogen gas adsorption technique (Rasmussen and Evans, 1987). The mercury porosimeter relies on a negative wetting coefficient resulting from a contact angle of about  $140^\circ$ . The mercury porosimetry technique is appropriate for pores with a radius in excess of 3.5 nm. Pores smaller than 100 nm can be measured using nitrogen gas adsorption techniques. The bulk density of a rock sample is the mass per unit volume of the sample. The bulk density is important for determining the neutron thermalization properties of a rock mass.

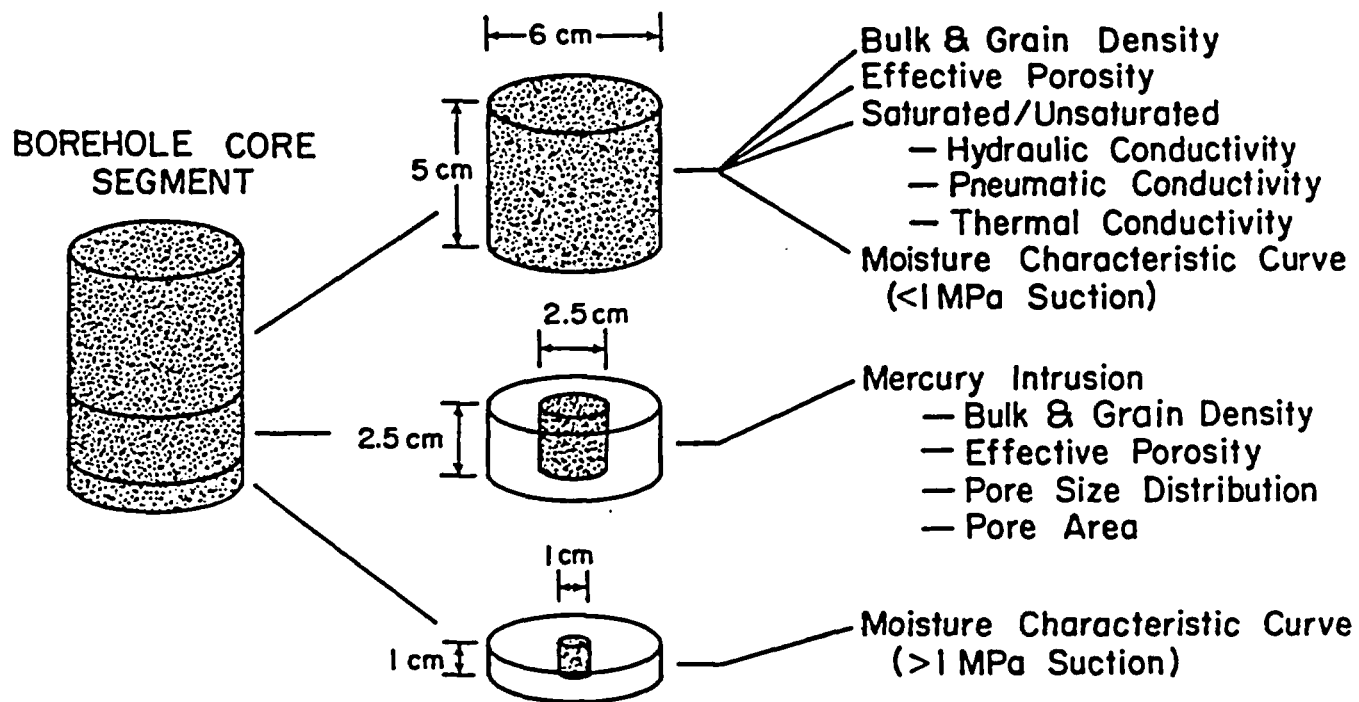


Figure 3: Core specimens used to obtain physical, hydraulic, pneumatic and thermal properties of rock samples obtained from the Apache Leap Tuff Site.

The effective porosity and the bulk density of a rock sample can be determined using the paraffin, water saturation, gravimetric and gamma ray attenuation methods (Rasmussen and Evans, 1987). The bulk density is defined as:

$$(2) \quad \rho_b = m_{\text{dry}} / V$$

where

$\rho_b$  bulk density of the sample,  $\text{kg/m}^3$ ;  
 $m_{\text{dry}}$  mass of oven dried sample, kg; and  
 $V$  volume of the sample,  $\text{m}^3$ .

If the sample is a regular solid, then the sample volume is found by measuring the physical dimensions of the sample. If the sample is not regular, it is saturated under vacuum and the saturated mass is recorded. The sample is then suspended by a fine wire and immersed in water within a beaker. The difference in mass between the beaker with the suspended sample and without the sample is the suspended sample mass. The volume of the sample is determined using:

$$(3) \quad V = (m_{\text{sat}} - m_{\text{sus}}) / \rho$$

where

$m_{\text{sat}}$  mass of saturated sample, kg;  
 $m_{\text{sus}}$  mass of suspended, saturated sample, kg; and  
 $\rho$  density of water,  $\text{kg/m}^3$ .

The effective porosity,  $n_e$  (dimensionless), of the sample is estimated using:

$$(4) \quad n_e = (w_{\text{sat}} - w_{\text{dry}}) / \rho V$$

The residual rock density,  $\rho_s$  ( $\text{kg/m}^3$ ), which includes rock grains and isolated pores, is found using:

$$(5) \quad \rho_s = \rho_b / (1 - n_e)$$

The pore size distribution is determined using mercury intrusion. A rock sample is examined by intruding mercury into the sample at pressures ranging from 0 to 200 MPa (0 to 2000 bars). Because mercury is lithophobic, increasingly higher pressures are required to force mercury into smaller pores. By measuring the volume of mercury intruded into the sample as a function of pressure, a relationship between pore size and frequency can be determined. Mercury intrusion is also used to determine the pore surface area, rock core volume, total effective porosity, and residual rock density.

Mercury porosimetry is based on the phenomenon of capillary law which governs the penetration of liquids into small pores. Because mercury does not wet the surface of most substances, mercury must be forced into cracks and pores by applying an external pressure on the liquid. Washburn (1921) suggested how one could obtain a pore size distribution of a porous body by relating the pressure-volume relationship from mercury penetration data. The familiar capillary-rise equation (Washburn Equation) is:

$$(6) \quad h_c = 2 \gamma \cos \alpha / R$$

where

- $h_c$  capillary suction, Pa;
- $\gamma$  surface tension, Pa m;
- $\alpha$  contact angle, degrees; and
- R pore radius, m;

For a non-wetting liquid like mercury the contact angle is greater than 90° which results in a pressure term rather than a suction term as with water. The application of the intrusion method to porous media assumes that all pores are interconnected and connected to the exterior surface. By using the volume of mercury intruded at various pressures, the pore radius frequency function can be obtained. An additional estimate of the pore radius distribution can be obtained by releasing the pressure of the mercury and observing the amount of mercury extruded. Different pore structures trap mercury during extrusion because of the "ink well" effect, resulting in hysteretic effects.

Pore surface area is calculated from the amount of work expended in forcing mercury into the pores. The work required to fully saturate an area of a pore wall is given by:

$$(7) \quad dW = \gamma \cos \alpha \, dA = -h \, dV$$

where

- W work, N;
- A pore surface area,  $m^2$ ;
- h applied pressure, Pa; and
- V volume of mercury intruded,  $m^3$ .

The total pore area is calculated by integrating  $(h \, dV)$  from a volume of mercury corresponding to pores of minimum size to a volume of mercury corresponding to pores of maximum size.

A total of 42 samples in seven boreholes are present within the (10 x 10 x 30 m) volume (see Figure 2). The X-, Y-, and Z-block data are data from samples of the X-, Y-, and Z-3 boreholes, respectively. Table 3 shows the mean values for bulk density, porosity, and pore area obtained using the mercury porosimetry method for the samples from each block completed to date. Fifteen of eighteen samples were analyzed for both the X- and Y- blocks while the Z-block incorporates only four of six samples. The greater number of samples from the X- and Y- blocks may be one explanation for the difference in porosity between blocks. Another explanation for the difference may result from the influence of depth, with samples from the Z-block being all less than 10 m below land surface while samples from the other blocks extend to 30 m. The characterization of all samples so far has shown a trend toward increasing porosity with borehole depth.

Ninety percent of all samples exhibit a bimodal pore size distribution (see Figure 4). Further analysis should give a more precise definition of this distribution and the role it plays in affecting water retention and transmission.

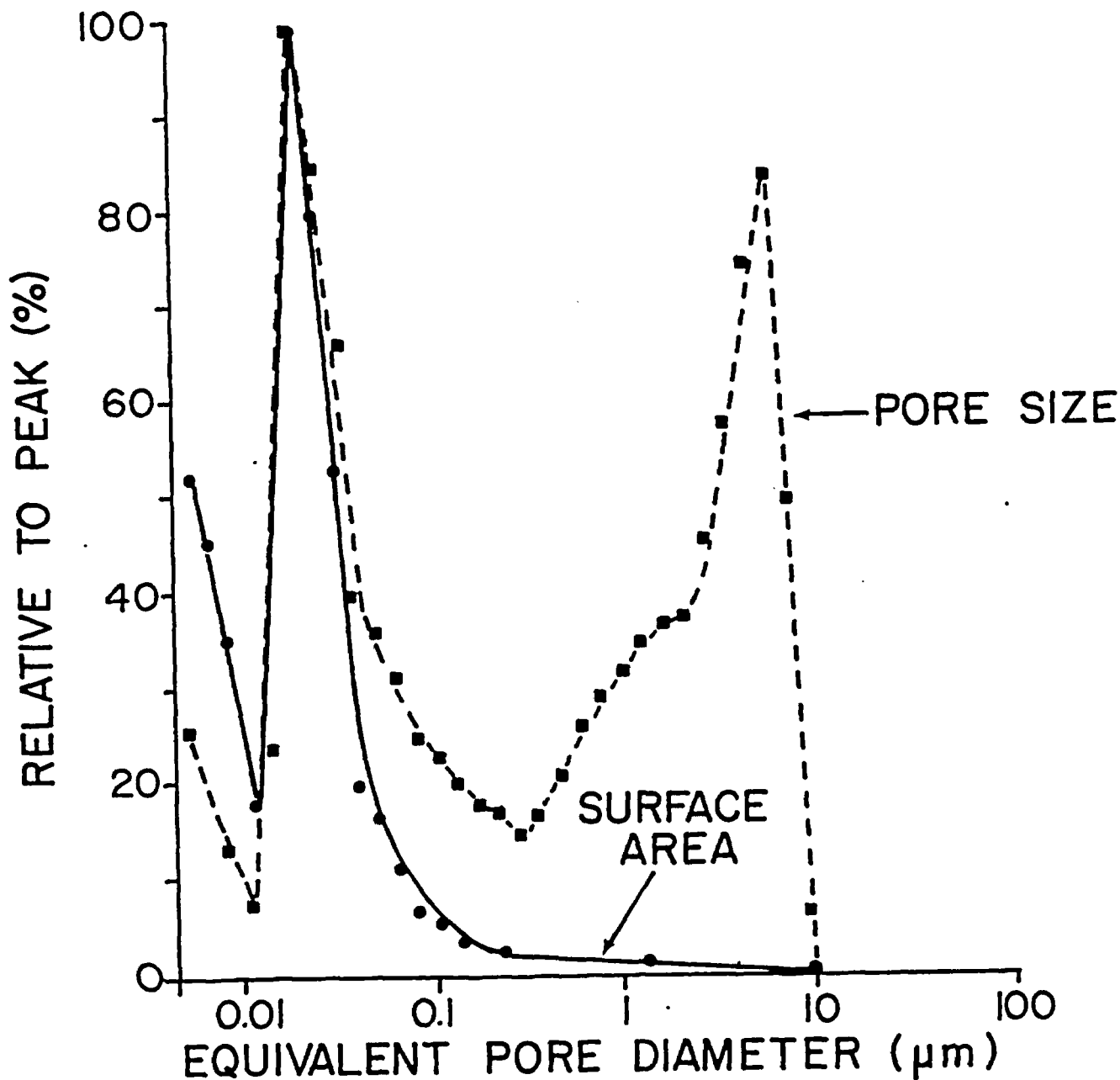


Figure 4: Representative pore size distribution of rock core sample obtained from the Apache Leap Tuff Site.

-----  
 Table 3: Mercury porosimetry results from Apache Leap Tuff Site.  
 -----

	Bulk Density (gm/cm <sup>3</sup> )		Porosity (percent)		Pore Area (m <sup>2</sup> /gm)	
	<u>mean</u>	<u>st.dev.</u>	<u>mean</u>	<u>st.dev.</u>	<u>mean</u>	<u>st.dev.</u>
X-Block	2.138	0.048	15.24	1.57	3.257	.231
Y-Block	2.132	0.036	15.07	2.27	2.949	.328
Z-Block	2.165	0.053	12.73	2.61	2.941	.403

-----

Saturated Hydraulic Conductivity

The saturated hydraulic conductivity is estimated using core segments which are saturated under vacuum and placed inside a permeameter (Figure 5). An inflatable packer within the permeameter is then pressurized to at least three bars to prevent bypassing of water between the core and the permeameter wall. Water is added to the upper surface of the rock core and a known pressure head of nitrogen gas, approximately one bar, is applied to the upper surface of the column of water which is in contact with the upper surface of the rock core. The outflow is measured by collecting water from a tube exiting the bottom of the permeameter. The hydraulic conductivity is determined using:

(8)  $K = Q L / A H$

where

- K hydraulic conductivity, m/s;
- Q volumetric flow through the core segment, m<sup>3</sup>/s;
- L length of the core segment, m;
- A area of the core segment, m<sup>2</sup>; and
- H hydraulic head difference across the core segment, m.

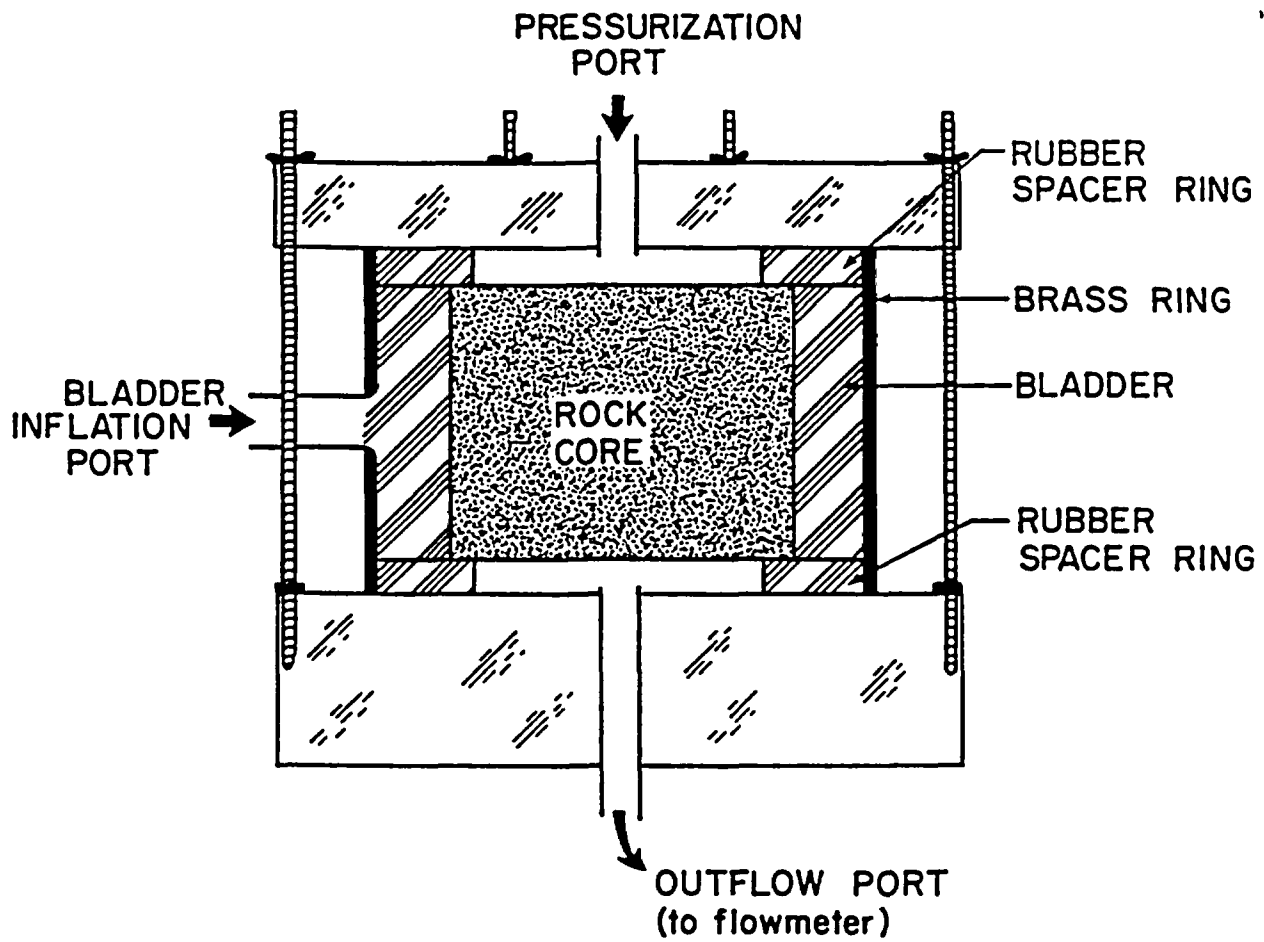


Figure 5: Experimental setup for determining saturated hydraulic conductivity and unsaturated pneumatic permeabilities.

The hydraulic head is computed from:

$$(8a) \quad H = p + (z_1 - z_2)$$

where

- p pressure head applied to the water surface, m;
- $z_1$  elevation of water surface above core, m; and
- $z_2$  elevation of the outlet point, m.

In addition to the hydraulic conductivity, the hydraulic permeability is also computed:

$$(9) \quad k_w = K \mu / \rho g$$

where

- $k_w$  hydraulic permeability,  $m^2$ ;
- $\mu$  dynamic viscosity, Pa s;
- $\rho$  fluid density,  $kg/m^3$ ; and
- g gravitational constant,  $m/s^2$ .

### Moisture Characteristic Curve and Unsaturated Hydraulic Conductivity Curves

The matrix moisture characteristic curve relates the fluid content of a rock sample to the ambient fluid potential within the matrix. This relationship can be generated by applying capillary theory to the pore size distribution or by using a pressure plate extractor or a Tempe pressure cell. Both the pressure plate extractor and the Tempe pressure cell are used to apply a known positive pressure to the sample and to measure the resulting liquid outflow.

The rock matrix moisture characteristic curve and unsaturated hydraulic conductivity curve between 0 and 1 bar (0 to 0.1 MPa) suction is obtained using the outflow method for the core segments. The outflow method uses a Tempe pressure cell with a 1 bar (0.1 MPa) porous plate to

provide an enclosed chamber within which an air pressure greater than atmospheric is applied (Figure 6). The excess air pressure is used to drive water from the sample through the porous plate, the rate of water flow and the total volume being used to determine the hydraulic diffusivity, moisture content, and the unsaturated hydraulic conductivity. Rahi (1986) provides a description of the apparatus and procedure used.

For suction between 1 and 10 bars (0.1 and 1 MPa) a porous plate assembly is used to determine the matrix moisture characteristic curve. The samples are placed on a porous plate within a pressure chamber and a constant pressure is applied. The samples are removed periodically and weighed until a constant weight is noted. The pressure within the chamber is increased to a prescribed level after a constant sample weight is obtained.

For suctions greater than approximately 10 bars (1 MPa), a thermocouple psychrometer (Rasmussen and Evans, 1987) is used to measure the moisture characteristic curve. The thermocouple psychrometer measures the wet-bulb depression of air that immediately surrounds a one by one centimeter rock cylinder. The wet-bulb depression is obtained by observing the temperature difference between a dry thermocouple and a thermocouple which has been immersed in de-ionized water and then removed. The wet-bulb depression is related to the water potential using tables calibrated from osmotic solutions. The water potential at various water contents is measured by allowing the rock sample to desaturate by evaporation in the atmosphere. The water content is determined using gravimetric procedures.

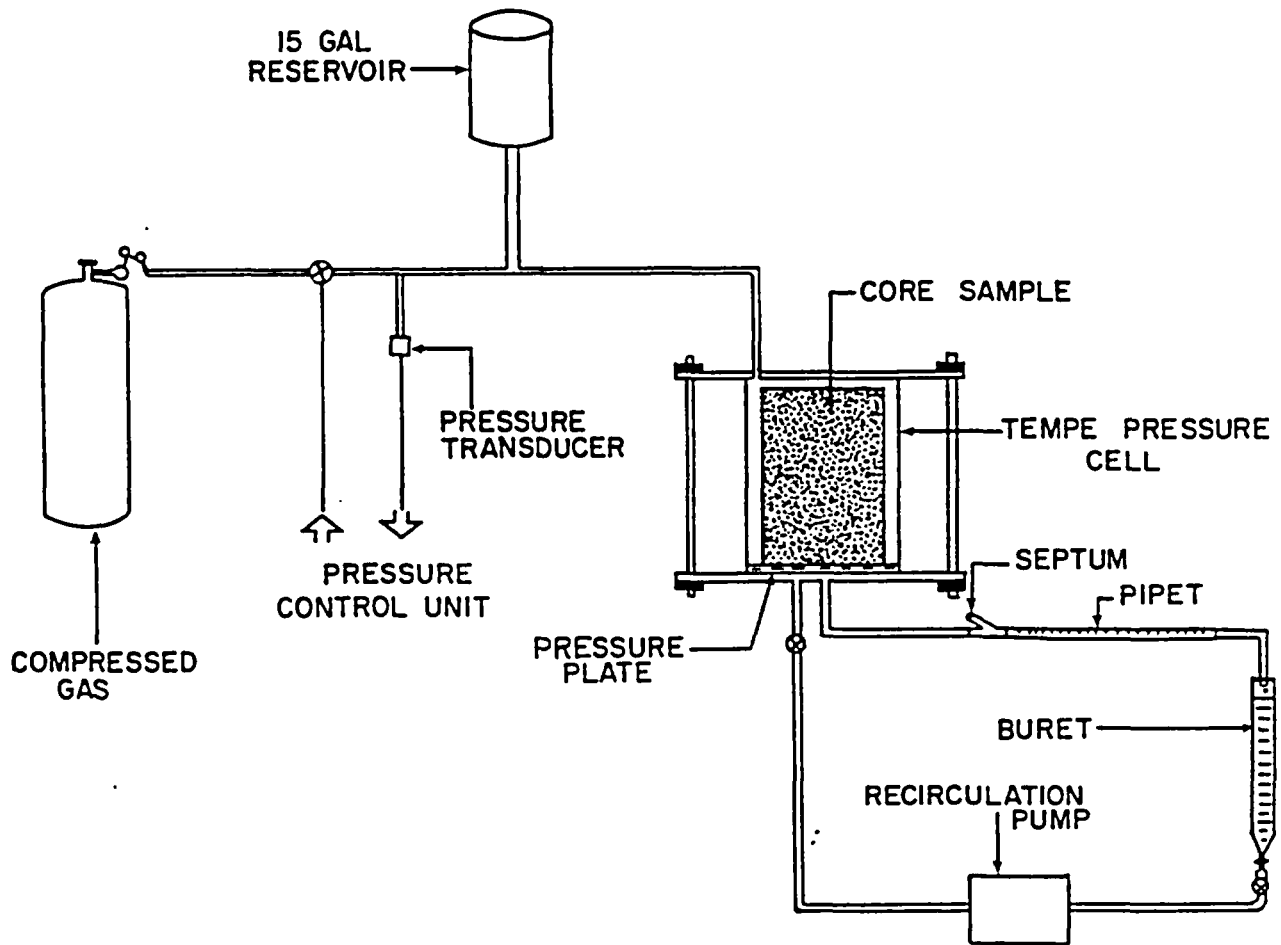


Figure 6: Experimental setup for the outflow method for determining unsaturated hydraulic conductivity.

Pneumatic Conductivity and Permeability

The pneumatic conductivity is obtained by employing the permeameter, illustrated previously in Figure 5. A core segment is desaturated to a prescribed suction or water content and then placed inside the permeameter with the packer inflated to prevent bypassing of air around the outside of the core. A known pressure gradient is applied longitudinally across the core segment and the air flow is measured using a soap bubble flow meter. The pneumatic conductivity is determined using the measured air flow, cross sectional area and core segment length. Because the air is compressible, the ideal gas law can be employed with the assumption of isothermal flow:

$$(10) \quad K_a = 2 Q L H_0 / A (H^2 - H_0^2)$$

where

- $K_a$  pneumatic conductivity, m/s;
- $H_0$  ambient atmospheric pressure head, m; and
- $H$  absolute pressure head applied to the upper rock surface, m.

The pneumatic permeability can be computed from air flow measurements using:

$$(11) \quad k_a = K_a \mu / \rho g$$

The unsaturated pneumatic permeability is obtained using the same method, except that prior to placing the core segment into the permeameter, the core segment is brought to the desired water content using a porous plate assembly.

The measured air permeability of a dry porous media is usually similar to the water permeability. However, for tuff cores the estimates are not similar due to slippage of air along the walls of pores. This phenomenon is known as the Klinkenberg effect (Green and Evans, 1987) and a correction factor, called here the Klinkenberg slip-flow coefficient, is used to correct for the differences in permeabilities:

$$(12) \quad k_a = k_w (1 + b/\bar{p})$$

where

- b     Klinkenberg slip-flow coefficient, Pa; and  
 $\bar{p}$     mean air pressure on the sample, Pa.

## Results

Table 4 summarizes parameter estimates for the 10 x 10 x 30 m rock volume. In all, 25 data points located within the sample region are available for analysis. Estimates of bulk density and effective matrix porosity are presented using two methods. Bulk density was measured using estimates of core volumes obtained from caliper measurements (i.e., BULK<sub>1</sub>), as well as from the displacement of rock samples in mercury (i.e., BULK<sub>2</sub>). The bulk density estimates compare favorably. The mean bulk density is 2.11 g/cm<sup>3</sup> and ranges from 1.99 to 2.18 using the first method. Grain densities of 2.34 to 2.61 with a mean of 2.55 are observed. A density of 2.65 is common for siliceous rocks, the difference perhaps being attributable to voids within the rock matrix which are not connected to exterior surfaces.

The effective matrix porosity was estimated using the difference in mass between an oven-dried sample and a vacuum saturated sample (column 1) and using the volume of mercury intruded within the sample (column 2). The effective porosity using the second method is always less than the value obtained using the first method. One explanation for this discrepancy may be that the mercury will not intrude into pores smaller than approximately 6 nm, while water will. If a large number of pores smaller than 6 nm exist within the rock matrix, the mercury porosimetry method will provide a biased estimate of matrix porosity. Estimated porosity averages 17.46 percent, but ranges from a low of 14.95 percent to a maximum of 20.38 percent using the first method.

The saturated hydraulic conductivity,  $K_{sat}$ , averages  $7.84 \times 10^{-16}$  m/s, and shows some variability between core samples, from a high of

$51.95 \times 10^{-16}$  m/s to a low of  $0.94 \times 10^{-16}$  m/s. The saturated hydraulic permeability,  $k_w$ , is estimated to be approximately  $7.30 \times 10^{-16}$  m<sup>2</sup>, while the air permeability for dry samples is several times larger,  $17.81 \times 10^{-16}$  m<sup>2</sup>. Estimates of the Klinkenberg slip-flow coefficient are presented as Figure 7. Note that the three estimates of the Klinkenberg slip flow coefficient all exhibit the same mode of approximately one bar. Herkelhath et al. (1983) report a value of 0.014 MPa for an unconsolidated porous material containing sand, silt and clay. Because the volcanic tuff used in the present experiments probably contains pores of smaller aperture than the porous material used in the Herkelhath et al. study, and also because slip flow is more pronounced at smaller apertures (Green and Evans, 1987), the increased estimate of the Klinkenberg coefficient used in the present study is plausible.

From Table 4 it is apparent that estimates of the pore surface area are quite stable, averaging about 3.13 m<sup>2</sup>/g. Because the estimated pore size distribution exhibits a bimodal property, the two mode pore diameters are presented as MPD1 and MPD2. From Table 4, the larger pores appear to concentrate around 3.13  $\mu$ m while the smaller pores are concentrated around 0.067  $\mu$ m.

Additional analyses are planned to complete the data set both within the 10 m x 10 m x 30 m block, and for all samples. Also, the thermal and the unsaturated hydraulic and pneumatic properties will be completed. The resulting data set will be analyzed for statistical correlations between parameters, as well as for spatial autocorrelations for each parameter. The data set will then be summarized in such a manner that stochastic and probabilistic modeling can be employed for the purpose of generating forecasts of flow and transport properties at scales larger than the field site.

Table 4: Summary of physical and hydraulic properties of rock core samples obtained from the Apache Leap Tuff Site.

Borehole Depth (m)	- Density (g/cm <sup>3</sup> ) -			Porosity (%)		K <sub>sat</sub>	k <sub>w</sub>	k <sub>a</sub>	k <sub>a</sub> /k <sub>w</sub>	Area	MPD1	MPD2	
	Bulk <sub>1</sub>	Bulk <sub>2</sub>	Grain	1	2	(m/s-16)	(m <sup>2</sup> x 10 <sup>-16</sup> )			(m <sup>2</sup> /g)	(μm)	(μm)	
X1	2.1	2.11	-	2.54	17.31	10.91	14.31	13.32	84.30	6.33	3.01	2.81	.070
	2.9	2.13	-	2.54	16.18	11.84	4.69	4.38	15.07	3.44	3.09	3.59	.070
	3.8	2.13	2.15	2.57	17.35	13.50	2.25	2.10	13.63	6.49	3.16	3.59	.090
	6.9	2.13	2.18	2.54	16.44	12.40	1.20	1.12	5.35	4.78	3.62	2.19	.070
	10.0	1.99	2.18	2.34	14.95	12.80	0.94	0.88	4.40	5.00	3.00	2.81	.070
	12.7	2.18	2.16	2.60	16.06	15.10	1.38	1.25	4.17	3.34	3.17	2.81	.055
	15.8	2.18	2.16	2.60	15.94	14.10	1.47	1.40	3.98	2.84	3.24	2.81	.055
X2	16.1	2.06	2.00	2.51	18.28	17.94	11.13	10.39	20.73	2.00	3.36	4.59	.070
	18.5	2.07	2.18	2.56	19.28	14.88	37.59	35.03	63.92	1.82	3.16	2.81	.055
	24.7	2.06	2.15	2.57	20.38	16.13	6.61	6.15	13.51	2.20	3.44	2.81	.055
	27.9	2.09	2.10	2.58	18.92	16.33	8.14	7.60	15.16	1.99	3.60	2.81	.055
	30.8	2.09	2.15	2.58	19.41	15.91	2.73	2.52	6.51	2.58	3.08	1.72	.043
X3	31.0	2.07	2.11	2.49	17.12	16.34	2.90	2.70	6.01	2.23	3.49	2.19	.055
	33.6	2.12	2.10	2.55	17.13	17.47	5.04	4.70	9.02	1.92	2.93	2.19	.055
	36.9	2.11	2.19	2.54	17.38	15.38	3.74	3.44	7.21	2.10	2.88	2.19	.043
Y1	1.9	2.17	2.12	2.61	16.62	13.70	1.73	1.58	6.59	4.17	3.26	3.59	.090
	3.3	2.14	2.15	2.55	16.49	11.90	4.61	4.28	35.18	8.22	3.32	2.81	.070
	4.1	2.13	2.11	2.57	16.74	11.70	3.58	3.35	17.89	5.34	-	-	-
	9.9	2.08	2.11	2.57	18.64	16.61	1.02	0.93	6.56	7.05	2.78	4.59	.055
	15.7	2.17	2.18	2.58	15.60	11.22	2.40	2.24	6.18	2.76	2.67	3.59	.055
Y2	15.3	2.11	2.11	2.57	18.04	15.94	3.63	3.40	9.74	2.86	3.08	3.59	.070
Z3	2.0	2.17	2.23	2.58	15.75	12.50	1.34	1.25	10.22	8.18	3.29	3.59	.070
	3.0	2.12	2.16	2.55	16.75	14.08	6.55	6.11	20.93	3.43	3.21	3.59	.070
	6.7	2.10	2.10	2.53	17.36	9.18	51.95	48.45	91.65	1.89	2.41	4.59	.055
	12.7	2.06	2.17	2.54	19.36	15.18	15.70	14.63	28.23	1.93	2.86	3.59	.070
MEAN	13.9	2.11	2.13	2.55	17.46	14.05	7.84	7.30	17.81	3.90	3.13	3.13	.067

Notes: Bulk density obtained from (1) caliper measure of samples and (2) mercury displacement.  
 Effective porosity obtained from (1) saturated minus oven-dry weight and (2) mercury intrusion.  
 MPD is Mode Pore Diameter. Two modes are listed because all samples displayed bimodal distributions.

NRC 04-86-114 - Progress Report (REV. 1) - NOVEMBER 1, 1987 - PAGE 23

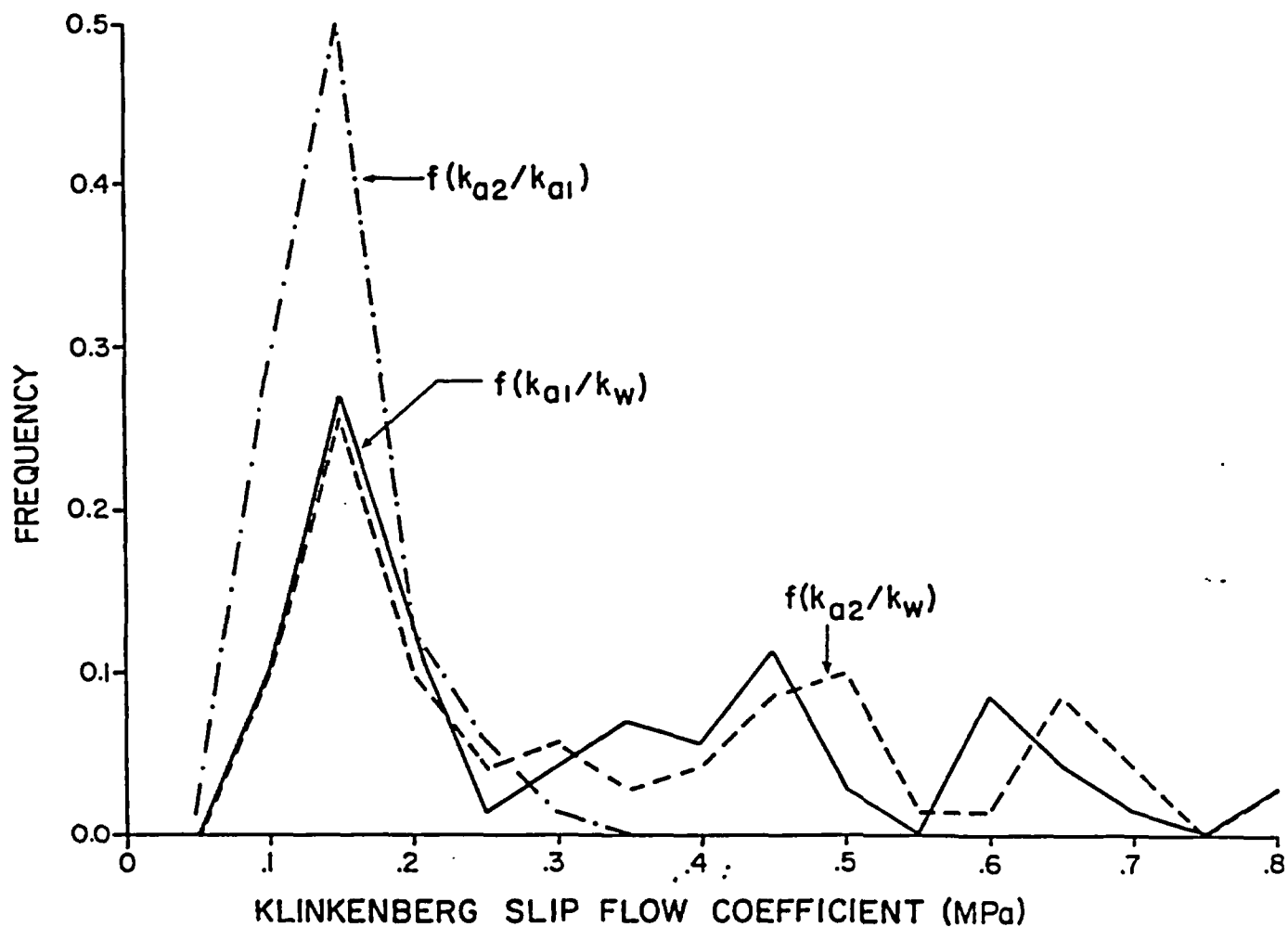


Figure 7: Relative frequency plot of the Klinkenberg slip flow coefficient estimated using high and low air pressure estimates of pneumatic permeability ( $k_{a2}/k_{a1}$ ), low air pressure estimates of pneumatic permeability and estimates hydraulic permeability ( $k_{a1}/k_w$ ), and high air pressure estimates of pneumatic permeability and estimates hydraulic permeability ( $k_{a2}/k_w$ ). Note that the mode for all estimates is approximately 0.1 MPa.

## Field Estimates of Precipitation, Infiltration and Deep Percolation

The disposition of incident precipitation is an important characterization parameter due to the importance of precipitation as the source term for subsurface flow and transport. The objective of this study is to provide data sets which will allow estimates of the recharge potential from atmospheric precipitation to be made. The data sets obtained from a field study of precipitation, infiltration and deep percolation are useful as input parameters in computer simulation models. The parameters are used to ascribe the upper boundary of the hydrogeologic system. To obtain meaningful characterization data sets, all elements of the water budget must be examined, including atmospheric precipitation, surface runoff, infiltration, surface storage, evapotranspiration, and deep percolation.

A field site located approximately 400 m to the west-northwest of the Apache Leap Tuff Site has been selected for performing a water budget analysis of small catchments (Figure 8). Two catchments have been identified, with areas of 1.73 and 0.24 ha (4.27 and 0.60 acres). The vegetation at the site is sparse, with over fifty percent exposed rock surfaces and little to no soil cover. Average slopes are 26 and 17 percent for the large and small catchments, respectively.

Precipitation at the site is measured using a tipping bucket rain gauge which provides rainfall intensity and total rainfall accumulation. The resolution of each bucket is 0.59 mm and the recording resolution is one minute. Additional rain collection devices will be used to measure the spatial variability of cumulative rainfall. The resolution of these devices is one mm. Expected rainfall intensities at the site are presented in Table 5. The determination of potential evapotranspiration will be accomplished using atmospheric temperature and relative humidity. Temperatures will be measured within a sheltered weather station using a thermistor with a precision of 0.02 °C. Relative humidity will be measured with a precision of one percent.

Runoff from the catchments will be measured in H-type flumes. The flumes will be instrumented with water level detectors using nitrogen

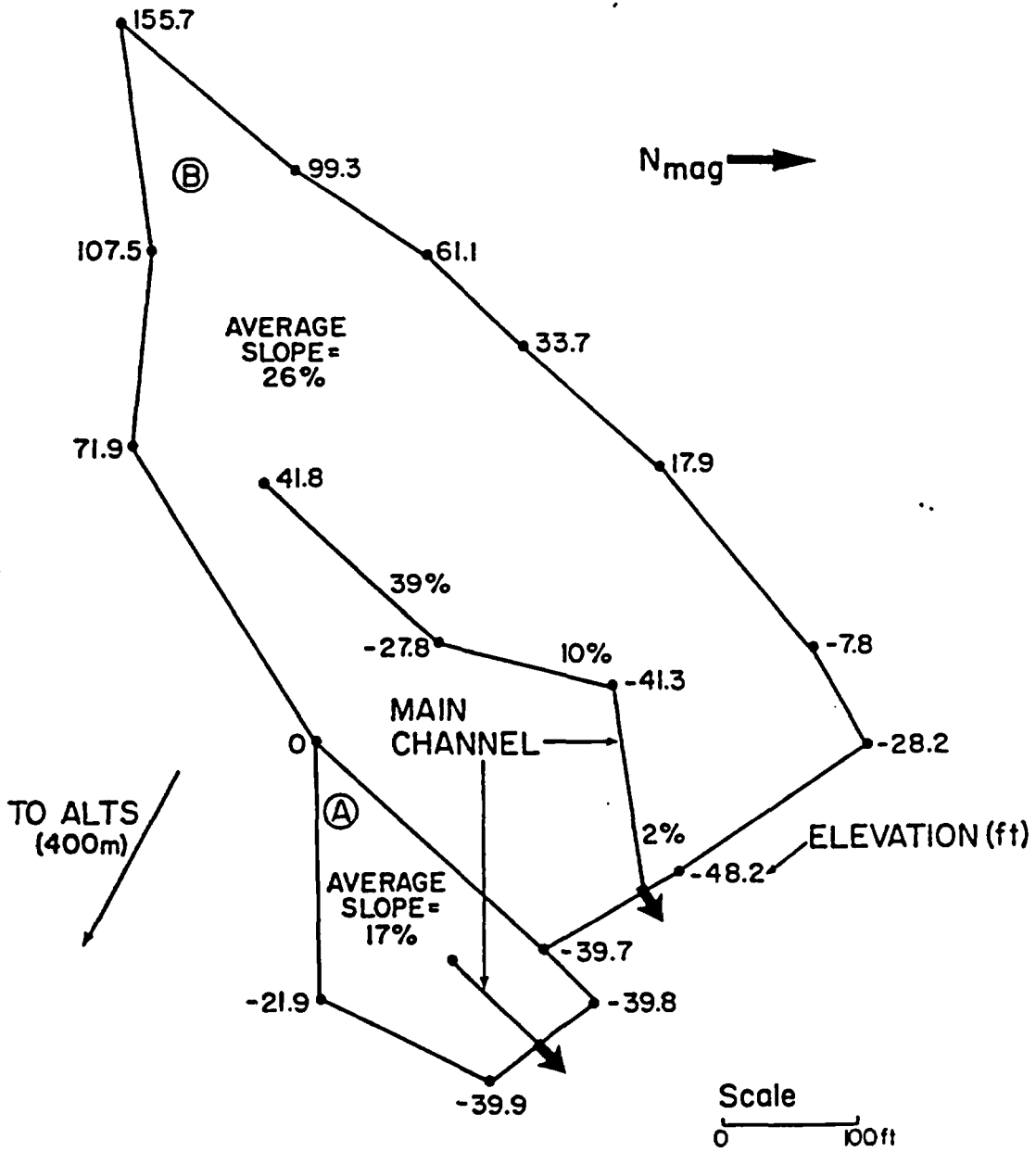


Figure 8: Plan view of small (A) and large (B) catchments to be used for water budget analyses of fractured rock water intake.

-----  
 Table 5: Expected maximum rainfall depths (inches) at the Apache Leap  
 Tuff Site. (Source: Miller et al., 1973)  
 -----

<u>Duration</u>	<u>Recurrence Interval</u>			
	<u>2 yr</u>	<u>5 yr</u>	<u>25 yr</u>	<u>100 yr</u>
15 min	0.70	0.74	0.97	1.21
30 min	0.96	1.03	1.34	1.68
1 hour	1.22	1.30	1.70	2.13
2 hour	1.42	1.64	2.21	2.70
3 hour	1.61	1.87	2.55	3.08
6 hour	1.80	2.30	3.20	3.80
12 hour	2.20	2.80	3.70	4.50
24 hour	2.50	3.25	4.20	5.25

-----

gas bubblers. Pressure transducers with an accuracy of one mm of water will be used to determine water level elevations at the control point within the flumes. Published rating tables are available which allow the determination of flow rates to within twelve liters per minute, corresponding to a uniform application of 0.04 and 0.30 mm/hr for the large and small catchments, respectively. This resolution is comparable to the resolution provided by the tipping bucket rain gauge for moderate and low intensity rainfall events.

The optimal estimates of water intake on the rock surface are made during low intensity precipitation events during periods when evapotranspiration demands are lowest. During all precipitation events, data concerning the rate and accumulation of precipitation, runoff rates, temperature, and humidity will be collected. Data acquisition and storage will be performed using a recorder with a sampling interval of ten seconds and a maximum storage capability of 5000 data points. Power to the recorder will be provided by a 55 amp-hour, twelve volt storage battery. Solar collectors with a maximum power output of 0.4 amps will be used to recharge the storage battery.

Literature Cited

- Davies, W., "Measurement of Thermal Conductivity and Diffusivity in an Unsaturated, Welded Tuff", M.S. Thesis, University of Arizona, 1987.
- Elder, A.N., "Theoretical Calibration of Neutron Gauges", M.S. Thesis, University of Arizona, In Progress.
- Green, R.T. and D.D. Evans, "Radionuclide Transport as Vapor through Unsaturated Fractured Rock", NUREG-CR-4654, 1987.
- Herkelhath, W.A., A.F. Moench, and C.F. O'Neal, "Laboratory Investigations of Steam Flow in a Porous Medium", Water Resour. Res., 19(4):931-937, 1983.
- Klavetter, E.A. and R.R. Peters, "An Evaluation of the Use of Mercury Porosimetry in Calculating Hydrologic Properties of Tuffs from Yucca Mountain", SAND86-0286, 1987.
- Miller, J.F., R.H. Frederick, and R.J. Tracey, "Precipitation-Frequency Atlas of the Western United States: VII - Arizona", NOAA, 1973.
- Rahi, K., "Hydraulic Conductivity Assessment for a Variably-Saturated Rock Matrix", M.S. Thesis, University of Arizona, 1986.
- Rasmussen, T.C. and D.D. Evans, "Unsaturated Flow and Transport through Fractured Rock - Related to High-Level Waste Repositories", NUREG/CR-4655, 1987.
- Washburn, E.W., "The Dynamics of Capillary Flow", Phys. Rev., 17(3):273-283, 374-375, 1921.

## Cumulative List of Project Publications

- Evans, D.D. and C. Huang., "Role of desaturation on transport through fractured rock, in Role of the Unsaturated Zone in Radioactive and Hazardous Waste Disposal, pp. 165-178, Ann Arbor, Science, 1983.
- Evans, D.D., Unsaturated flow and transport through fractured rock - related to high-level waste repositories, U.S. Nuclear Regulatory Commission, NUREG/CR-3206, 231 p, 1983.
- Huang, C. and D.D. Evans, A 3-dimensional computer model to simulate fluid flow and contaminant transport through a rock fracture system, U.S. Nuclear Regulatory Commission, NUREG/CR-4042, 109 p, 1985.
- Schrauf, T.W. and D.D. Evans, Relationship between the gas conductivity and geometry of a natural fracture, U.S. Nuclear Regulatory Commission, NUREG/CR-3680, 131 p, 1984.
- Green, R.T. and D.D. Evans, "Radionuclide transport as vapor through unsaturated fractured rocks", in Memoirs of Congress on Hydrology of Rocks of Low Permeability, International Association of Hydrogeologists, Tucson, Az., 17(1): 254-266, 1985.
- Rasmussen, T.C., C. Huang, and D.D. Evans, "Numerical experiments on artificially - generated, three-dimensional fracture networks: an examination of scale and aggregation effects", in Memoirs of Congress on Hydrology of Rocks of Low Permeability, International Association of Hydrogeologists, Tucson, Az., 17(2):676-682, 1985.
- Green, R.T., W.L. Filipone, and D.D. Evans, "Effect of electric fields on vapor transport near a high-level waste canister", in Proceedings of the International Symposium on Coupled Processes Affecting the Performance of a Nuclear Waste Repository, Lawrence Berkeley Laboratories, September 18-20, 1985.
- Rasmussen, T.C., "Improved site characterization using multiple approaches", in Proceedings of Symposium on groundwater flow and transport modeling for performance assessment of deep geologic disposal of radioactive waste: A critical evaluation of the state of the art, Albuquerque, NM, May 20, NUREG/CP-0079, pp. 101-113, 1986.

Schrauf, T.W. and D.D. Evans, "Laboratory studies of gas flow through a single natural fracture", Water Resour. Res., 22(7):1038-1050, 1986.

Kilbury, R.K., T.C. Rasmussen, D.D. Evans, and A.W. Warrick, "Water and air intake measurement technique for fractured rock surfaces", Water Resour. Res., 22(10):1431-1443, 1986.

Green, R.T. and D.D. Evans, Radionuclide transport as vapor through unsaturated fractured rock, NUREG-CR-4654, 1987.

Rasmussen, T.C. and D.D. Evans, Unsaturated flow and transport through fractured rock - Related to high-level waste repositories, NUREG/CR-4655, 1987.

Rasmussen, T.C., "Meso-scale estimates of unsaturated fractured rock fluid flow parameters", in Farmer, I.W., J.J.K. Daemen, C.S. Desai, C.E. Glass and S.P. Neuman (Eds.), Rock mechanics: Proceedings of the 28th US Symposium, University of Arizona, Tucson, June 29-July 1, A.A. Balkema, p. 525-532, 1987.

Rasmussen, T.C., "Computer simulation of steady fluid flow and solute transport through three-dimensional networks of variably saturated, discrete fractures", in Evans, D.D. and T.J. Nicholson (Eds.), Flow and transport through unsaturated fractured rock, AGU Geophysical Monograph 39, 1987

Presented Papers

- Cullinan, S.R., C. Huang, and D.D. Evans, Non-isothermal vapor transport in a single unsaturated rock fracture, abstract, Amer. Geophys. Union, EOS, v. 63, no. 45, p.934, 1982.
- Evans, D.D., R.C. Trautz, J.W. Andrews, and D.E. Earp, Water flow in and unsaturated fractured rock: a case study, abstract, Amer. Geophys. Union, EOS, v. 64. no. 18, p. 228, 1983.
- Earp, D.E., D.D. Evans, and C. Huang, An osmotic tensiometer for measuring pressure head in unsaturated fractured rock, abstract, Amer. Geophys. Union, EOS, v. 64, no. 18, p.228, 1983.
- Huang, C. and D.D. Evans, Modeling flow in unsaturated, fractured rock formations with application to nuclear waste repositories, abstract, Amer. Geophys. Union, EOS, v.64. no. 18, p. 229, 1983.
- Schrauf, T.W. and D.D. Evans, Laboratory studies of gas flow through a single natural fracture, abstract, Amer. Geophys. Union, EOS, v. 64, no. 45, p. 704, 1983.
- Green, R.T. and D.D. Evans, Radionuclide transport as Vapor through unsaturated fractured rock, abstract, Amer. Geophys. Union, EOS, v. 65, no. 45, p.881, 1984.
- Rasmussen, T.C., Improved site characterization using multiple approaches, presented at Symposium on groundwater flow and transport modeling for performance assessment of deep geologic disposal of radioactive waste: A critical evaluation of the state of the art, Albuquerque, NM, May 20, 1985.
- Kilbury, R.K., T.C. Rasmussen, and D.D. Evans, Water intake across the atmosphere-earth boundary into a fractured rock system, abstract, Amer. Geophys. Union, EOS, v. 66, no. 18, p.266, 1985.
- Nicholson, T.J., and D.D. Evans, High level radioactive waste repository site characterization: unsaturated zone, abstract, Amer. Geophys. Union, EOS, v. 66, no. 18, p. 269, 1985.
- Rasmussen, T.C., and D.D. Evans, Three-dimensional computer modeling of discrete fracture networks: application to unsaturated media, abstract, Amer. Geophys. Union, EOS, v.66, no. 18, p.275, 1985.

Green, R.T., W.L. Filipone, and D.D. Evans, Effect of electric fields on vapor transport near a high-level waste canister, International Symposium on Coupled Processes Affecting the Performance of a Nuclear Waste Repository, Lawrence Berkeley Laboratories, September 18-20, 1985.

Rasmussen, T.C., and D.D. Evans, Three-dimensional computer model of discrete fracture networks incorporating matrix diffusion, abstract, Amer. Geophys. Union, EOS, v.66, no. 46, 1985.

Rasmussen, T.C., Modeling of three-dimensional fracture networks, presented at Unsaturated rock/contaminant transport workshop II, Tucson, AZ, January 8, 1986.

#### Theses and Dissertations

Cullinan, Steve R., Non-Isothermal Vapor Transport in a Single Unsaturated Rock Fracture, May 1983, Hydrology.

Andrews, Jon W., Water Content of Unsaturated, Fractured, Crystalline Rocks from Electrical Resistivity and Neutron Logging, December 1983, Hydrology.

Schrauf, Todd W., Relationship Between the Gas Conductivity and Geometry of a Natural Fracture, May 1984, Hydrology.

Trautz, Robert C., Rock Fracture Aperture and Gas Conductivity Measurements In Situ, December 1984, Hydrology.

Green, Ron T., Transport of Radionuclides as Vapor in Unsaturated Fractured Rock, December 1985, Hydrology.

Amter, Steven, Injection-Recovery Techniques for Vacuum Lysimeter Sampling in Highly Unsaturated Media, May 1987, Hydrology.

Amutis, Rikki, The Application of Thermoelectric Cooling Techniques to Sampling and Detection of Solutes in Unsaturated Fractured Rock, December 1987, Hydrology.

Anderson, Ingrid, Measurement of Unsaturated Rock-Water Potential In Situ, May 1987, Hydrology.

- Davies, Bill, Measurement of Thermal Conductivity and Diffusivity in an Unsaturated, Welded Tuff, May 1987, Hydrology.
- Rahi, Khayyun, Hydraulic Conductivity Assessment for a Variably-Saturated Rock Matrix, December 1986, Hydrology.
- Roberts, Mary, Volatile Fluorocarbon Tracers for Monitoring Water Movement in the Unsaturated Zone, May 1987, Hydrology.
- Weber, Dan, Mineralogic, Isotopic and Spatial Properties of Fractures in an Unsaturated, Partially-Welded Tuff near Superior, Arizona, May 1987, Hydrology.
- Elder, Alexander N., Theoretical Calibration of Neutron Gauges, In Progress, Hydrology.
- Rasmussen, Todd Christian, Fluid Flow and Solute Transport Through Three-Dimensional Networks of Variably-Saturated Discrete Fractures, In Progress, Hydrology.
- Goering, Tim, Use of Fluorescent Dyes as Tracers in Unsaturated, Fractured Rock, In Progress, Hydrology.
- Mathews, Daniel, Thermally Induced Counter-Current Flow in Unsaturated Rock, In Progress, Hydrology.
- Brown, Steve R., Estimation of Net Recharge Through Thick Unsaturated Zones by Profile Modeling of Saturated Flow Dynamics, In Progress, Hydrology.